Available online at www.sciencedirect.com

ScienceDirect

Ceramics International 40 (2014) 4187–4191

CERAMICS INTERNATIONAL

www.elsevier.com/locate/ceramint

Suppression of 3D mobility of carrier and superconductivity by Y^{+3} substitution in $Cu_{0.5}Tl_{0.5}Ba_2(Ca_{2-x}Y_x)Cu_3O_{10-\delta}$ samples

M. Mumtaz[a,b,*], Nawazish A. Khan[b], Saleem Abbas[b], Khurram Shehzad[c]

[a]Materials Research Laboratory, Department of Physics FBAS, International Islamic University (IIU), Islamabad 44000, Pakistan
[b]Materials Science Laboratory, Department of Physics, Quaid-i-Azam University, Islamabad 45320, Pakistan
[c]Department of Engineering Mechanics, Center for Nano and Micro Mechanics, Tsinghua University, Beijing 100084, China

Received 21 May 2013; received in revised form 25 July 2013; accepted 19 August 2013
Available online 17 September 2013

Abstract

Bulk $Cu_{0.5}Tl_{0.5}Ba_2(Ca_{2-x}Y_x)Cu_3O_{10-\delta}$ superconductor ceramic samples were synthesized by the conventional solid-state method and characterized by X-ray diffraction, dc-resistivity, ac-susceptibility and Fourier Transform Infrared spectroscopy. The main purpose of this study was to investigate the role of charge carriers and the effect of Y substitution at Ca sites in between the CuO_2 planes on superconductivity. The superconducting properties are suppressed by Y substitution at Ca sites in between the CuO_2 planes of $Cu_{0.5}Tl_{0.5}Ba_2(Ca_{2-x}Y_x)Cu_3O_{10-\delta}$ samples. It is most likely that Y^{3+} may create correlated domains in between the CuO_2 planes and localizes the carriers, which lowers the diamagnetic screening and suppresses the superconductivity. Therefore, cationic substitution reduces the three dimensional (3D) mobility of carriers, resulting in the reduction of the Fermi vector and velocity of the carriers, which in turn suppresses the superconducting properties of the material.

Keywords: $Cu_{0.5}Tl_{0.5}Ba_2(Ca_{2-x}Y_x)Cu_3O_{10-\delta}$ superconductor; Substitution; Localization; Mobility of carriers

1. Introduction

The complexity of high T_c superconductors requires the understanding of charge transfer mechanism and mobility of the carriers. The mechanism of superconductivity in cuprates is still unclear but there is a common consensus that the observed variation in T_c partially depends upon optimum carriers concentration, their mobility along the *c*-axis and also on the conductivity of the charge reservoir layer. In order to increase the mobility of carriers along the *c*-axis, the inter-CuO_2-planes coupling in $Cu_{0.5}Tl_{0.5}Ba_2Ca_2Cu_3O_{10-\delta}$ superconductors was improved by Be and Mg doping at Ca sites in between the CuO_2 planes [1–4]. The superconducting properties are significantly enhanced by Be and Mg-doping at Ca sites in $Cu_{0.5}Tl_{0.5}Ba_2(Ca_{2-y}M_y)Cu_3O_{10-\delta}$; (M=Be, Mg) superconductors. Both these elements (Be and Mg) of the same +2 oxidation state have smaller size, higher electronegativity values than that of replaced Ca atom. Decrease in the *c*-axis length has been observed in Be and Mg-doped samples [1–4], which is the reminiscent of increased coherence length (ξ_c) and enhanced mobility of carriers along the *c*-axis due to improved inter-CuO_2-planes coupling. We doped Y^{+3} at Ca^{+2} sites in between the CuO_2 planes of $Cu_{0.5}Tl_{0.5}Ba_2(Ca_{2-x}Y_x)Cu_3O_{10-\delta}$ superconductors in order to look into the role of charge state of the doped elements on superconductivity. In the literature, the effects of Y-doping at Ca sites in different high T_c superconducting families are found to be poisonous for superconducting properties [5–12]. Different arguments were given to explain the fatal effects of Y substitution on superconductivity.

Since the atomic and covalent radii of Y are smaller than those of Ca, the charge state of Y^{3+} is greater than that of Ca^{2+}. The doping of Y at the Ca sites would help in understanding the role of enhanced charge state of doped elements in between the CuO_2 planes on the mechanism of high T_c superconductivity. The prime objective of Y-doping was to improve the inter-CuO_2-planes coupling and to enhance

*Corresponding author at: Materials Research Laboratory, Department of Physics FBAS, International Islamic University (IIU), Islamabad 44000, Pakistan. Tel.: +92 51 9019715 (office); fax: +92 51 9210256.
E-mail address: mmumtaz75@yahoo.com (M. Mumtaz).

0272-8842/$ - see front matter
http://dx.doi.org/10.1016/j.ceramint.2013.08.076

the superconducting properties of $Cu_{0.5}Tl_{0.5}Ba_2(Ca_{2-x}Y_x)Cu_3O_{10-\delta}$ material [13]. It was expected that Y^{+3} having smaller size and higher electronegativity than Ca^{+2} would improve the inter-CuO_2-planes coupling and would increase the three dimensional (3D) conductivity of carriers in the bulk materials. But to our surprise, we got the results other way round i.e. superconducting properties (T_c, magnitude of diamagnetism, etc.) are suppressed with the increase of Y-content in $Cu_{0.5}Tl_{0.5}Ba_2(Ca_{2-x}Y_x)Cu_3O_{10-\delta}$ samples. These unexpected results have shed light on the role of charge state of doped atom on the mobility of carriers. These results showed that Y-doping has influenced the anisotropy through the variation of carriers concentration [14]. It was observed in previous studies that the substitution of Y^{3+} decreases the average valance state of Cu (or hole concentration) resulting in the decrease of T_c [5,6,15,16]. It was found by Yamanaka et al. [7] that when the hole concentration decreases by Y substitution at Ca sites in $Bi_2Sr_2Ca_{1-x}Y_xCu_2O_{8-y}$ superconductor, the superconducting gap increases and T_c decreases. Mumtaz et al. [17] also studied the variation of superconducting properties with the change of hole concentration in CuTl-1223 superconductor by means of cationic substitution.

2. Experimental details

We have synthesized $Cu_{0.5}Tl_{0.5}Ba_2(Ca_{2-x}Y_x)Cu_3O_{10-\delta}$ superconducting samples by the solid-state method accomplished in two stages. In the first stage $Cu_{0.5}Ba_2(Ca_{2-x}Y_x)Cu_3O_{10-\delta}$ precursor material was prepared by thoroughly mixing of $Ba(NO_3)_2$, $Ca(NO_3)_2$, $Cu_2(CN)_2$ and Y_2O_3 in a quartz mortar and pestle in appropriate ratios. The mixed material was ground for about 1 h and then fired thrice at 860 °C in a quartz boat for more than 24 h followed by furnace cooling to room temperature. The material was ground for 1 h after each time 24 h firing. In the second stage, appropriate amount of Tl_2O_3 was added to $Cu_{0.5}Ba_2(Ca_{2-x}Y_x)Cu_3O_{10-\delta}$ precursor material to obtain $Cu_{0.5}Tl_{0.5}Ba_2(Ca_{2-x}Y_x)Cu_3O_{10-\delta}$ samples as final composition. Thoroughly mixed material with Tl_2O_3 was palletized under 3.8 t/cm^2 pressure. The pellets were then carefully enclosed in gold capsules and sintered for 10 min at 860 °C followed by quenching to room temperature. The samples were characterized by X-ray diffraction (XRD), dc-resistivity, ac-susceptibility, and Fourier Transform Infrared (FTIR) spectroscopy measurements. The conventional four probe dc-resistivity measurement setup was used to measure the temperature dependent dc-resistivity (ρ) of the samples. Liquid nitrogen was used for low temperature measurements up to 77 K. The samples holder containing the sample was put into the liquid nitrogen container slowly and the temperature was monitored at the rate of 1 K/min. The ac-susceptibility was measured by using a lock-in amplifier at 270 Hz lock-in frequency. The mutual induction method was employed to determine the diamagnetic signal. Liquid nitrogen was also used for the ac-susceptibility measurements at low temperature up to 77 K.

3. Results and discussion

X-ray diffraction (XRD) scans of $Cu_{0.5}Tl_{0.5}Ba_2(Ca_{2-x}Y_x)Cu_3O_{10-\delta}$ ($x=0$, 0.015, 0.025, 0.05, and 0.075) samples are shown in Fig. 1. Most of the diffraction peaks observed in XRD scans are indexed for orthorhombic crystal structure by using the Pmmm space group. The cell parameters are calculated from the XRD analysis using computer software (crystal) and the systematic increase in the axes lengths was observed after Y-doping in $Cu_{0.5}Tl_{0.5}Ba_2(Ca_{2-x}Y_x)Cu_3O_{10-\delta}$ ($x=0$, 0.015, 0.025, 0.05, and 0.075) samples. The unit cell volume determined from the axes lengths of $Cu_{0.5}Tl_{0.5}Ba_2(Ca_{2-x}Y_x)Cu_3O_{10-\delta}$ superconductor samples are 253.39, 258.11, 259.27, 264.04 and 265.04 Å^3 for $x=0$, 0.015, 0.025, 0.05, and 0.075 respectively. The unit cell volume also systematically increases with increasing Y-doping concentration in the samples. The density is decreased in all Y-doped samples; more suppression in the density is observed for

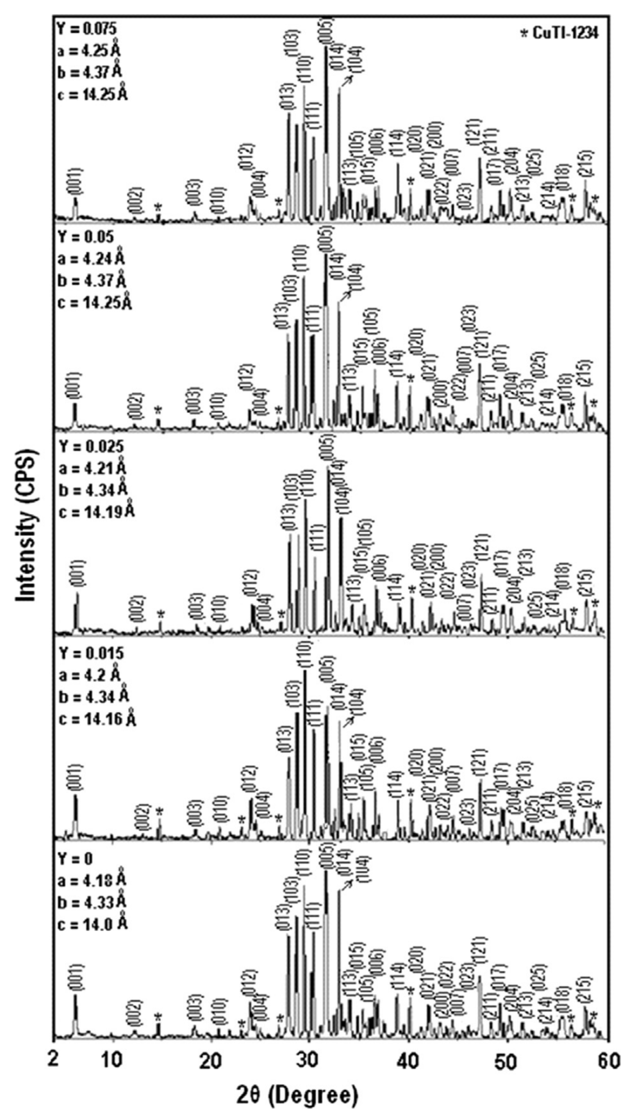

Fig. 1. X-ray diffraction (XRD) scans of $Cu_{0.5}Tl_{0.5}Ba_2(Ca_{2-x}Y_x)Cu_3O_{10-\delta}$ ($x=0$, 0.015, 0.025, 0.05, and 0.075) superconductor samples.

Table 1
A summary of resistivity, density and XRD of $Cu_{0.5}Tl_{0.5}Ba_2(Ca_{2-x}Y_x)Cu_3O_{10-\delta}$ samples for $x=0$, 0.015, 0.025, 0.05, and 0.0 75.

$(Tl_{1-x}Y_x)Ba_2Ca_2Cu_3O_{10-\delta}$	ρ (Ω cm) at 290 K	T_c^{onset} (K)	T_c ($R=0$) (K)	Density(g/cm^3)	Unit cell parameters (*a–c*-axis) (Å)	Residual resistivity
$x=0$	0.397	109	96	2.97	$a=4.18$, $b=4.33$, $c=14.00$	0.17
$x=0.015$	0.488	118	86	2.25	$a=4.2$, $b=4.34$, $c=14.16$	0.34
$x=0.025$	0.927	117	87	1.77	$a=4.21$, $b=4.34$, $c=14.19$	0. 6
$x=0.05$	0.614	112	78	1.26	$a=4.24$, $b=4.37$, $c=14.25$	0.04
$x=0.075$	1.001	114	77	1.12	$a=4.25$, $b=4.37$, $c=14.25$	0.78

$x=0.025$, 0.05, and 0.075, see Table 1. The density of the samples presented in the manuscript is calculated theoretically as

$$\rho = M/V_c$$

where M is the molecular weight of the elements in the unit cell and V_c is the volume of the unit cell. The increase in the volume of the unit cell after Y-doping causes the decrease in the density of the samples. The ionic size of Y^{3+} is smaller than Ca^{2+} but the volume of the unit cell has been increased after Y-doping. Therefore, the decrease in mass per unit volume (i.e. density) is very obvious after Y-doping. It was found that mechanical properties after Y-doping at Ca sites in $Bi_2Sr_2Ca_{1-x}Y_xCu_2O_{8-\delta}$ superconductor samples were improved showing the better connections of grains in the material. But the density of the samples was also found to be reduced in Y-doped $Bi_2Sr_2Ca_{1-x}Y_xCu_2O_{8-\delta}$ superconductor samples owing to the presence of pores [8]. The microhardness of these samples was also decreased after Y-doping, which is also the evidence of the presence of pores and reduction of density of the samples.

The influence of increase in the *c*-axis length and unit cell volume can be seen in the FTIR absorption spectra of these samples. The phonon modes related to the oxygen atoms in the unit cell observed by FTIR absorption spectra of $Cu_{0.5}Tl_{0.5}Ba_2(Ca_{2-x}Y_x)Cu_3O_{10-\delta}$ ($x=0$, 0.015, 0.025, 0.05, and 0.075) superconductor samples are shown in Fig. 2. The apical oxygen modes of type Cu(2)–O_A–Tl are observed around 540, 542, 541, 545, and 545 cm^{-1} and apical oxygen modes of type Cu(2)–O_A–Cu(1) are observed around 420, 422–450, 423–457, 417–457, and 420–456 cm^{-1} in $Cu_{0.5}Tl_{0.5}Ba_2(Ca_{2-x}Y_x)Cu_3O_{10-\delta}$ samples for $x=0$, 0.015, 0.025, 0.05, and 0.075, respectively. The planar oxygen modes in $Cu_{0.5}Tl_{0.5}Ba_2(Ca_{2-x}Y_x)Cu_3O_{10-\delta}$ samples are observed around 579, 578, 578, 577, and 569 cm^{-1} for $x=0$, 0.015, 0.025, 0.05, and 0.075, respectively. These planar oxygen modes are slightly softened after Y-doping at Ca sites in $Cu_{0.5}Tl_{0.5}Ba_2(Ca_{2-x}Y_x)Cu_3O_{10-\delta}$ superconductor samples. The substitution of Y at Ca sites in between the CuO_2 planes promotes the expansion of the lattice and increases the bond distances, which results in the softening of the CuO_2 planar oxygen modes. The expansion of distances between the CuO_2 planes develops the pressure on the apical oxygen bond distances and as a result apical oxygen modes of types Cu(2)–O_A–Tl and Cu(2)–O_A–Cu(1) are slightly shifted to higher wavenumbers (i.e. become hardened) due to reduction of apical oxygen bond lengths with the Y-doping at Ca sites in $Cu_{0.5}Tl_{0.5}Ba_2(Ca_{2-x}Y_x)Cu_3O_{10-\delta}$ superconductor samples.

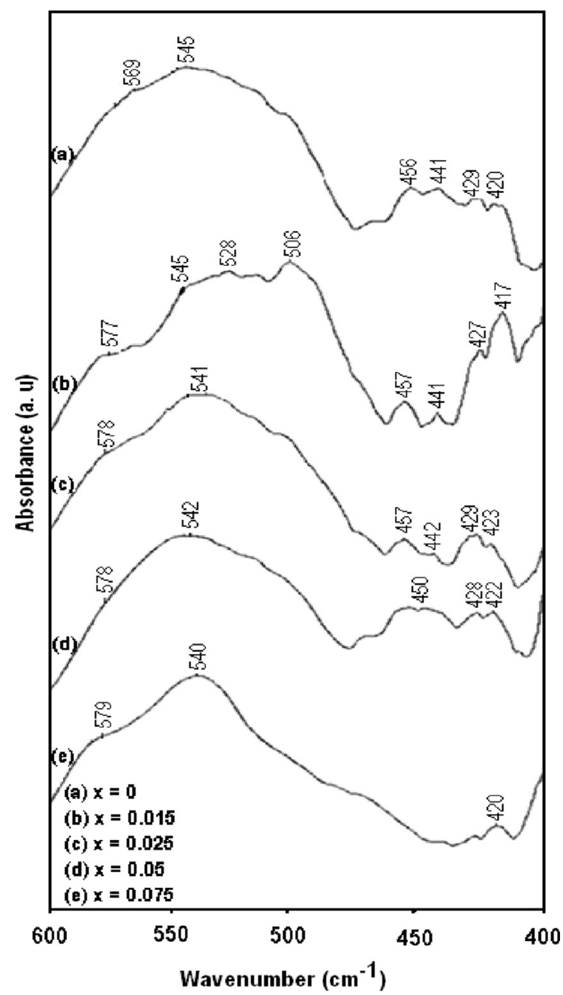

Fig. 2. The FTIR absorption spectra of $Cu_{0.5}Tl_{0.5}Ba_2(Ca_{2-x}Y_x)Cu_3O_{10-\delta}$ ($x=0$, 0.015, 0.025, 0.05, and 0.075) superconductor samples.

The electrical dc-resistivity as a function of temperature between 77 and 300 K and residual resistivity measurements are carried out to investigate the effects of Y substitution on superconducting properties of $Cu_{0.5}Tl_{0.5}Ba_2(Ca_{2-x}Y_x)Cu_3O_{10-\delta}$ samples as shown in Fig. 3. The variation of T_c ($R=0$) versus Y-content in $Cu_{0.5}Tl_{0.5}Ba_2(Ca_{2-x}Y_x)Cu_3O_{10-\delta}$ samples are plotted in Fig. 4. We have observed metallic

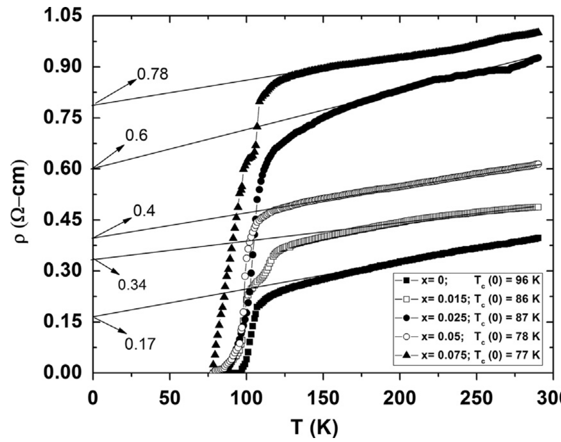

Fig. 3. The resistivity versus temperature measurements and residual resistivity of $Cu_{0.5}Tl_{0.5}Ba_2(Ca_{2-x}Y_x)Cu_3O_{10-\delta}$ (x=0, 0.015, 0.025, 0.05, and 0.075) superconductor samples.

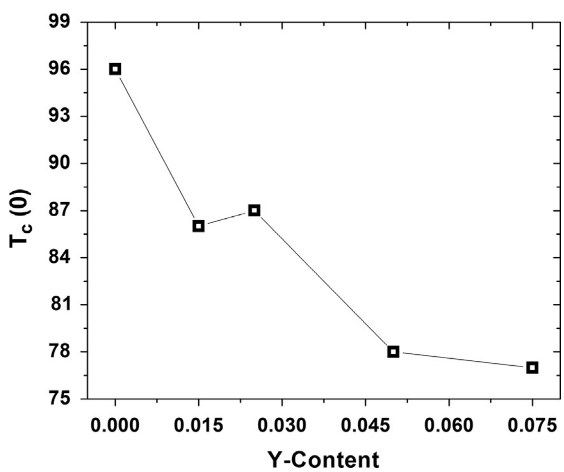

Fig. 4. Variation in T_c (R=0) versus Y-content in $Cu_{0.5}Tl_{0.5}Ba_2(Ca_{2-x}Y_x)Cu_3O_{10-\delta}$ (x=0, 0.015, 0.025, 0.05, and 0.075) superconductor samples.

behavior in the dc-resistivity data from room temperature down to onset of superconductivity. The onset of superconductivity temperature {T_c^{onset} (K)} is observed around 109, 118, 117, 106, and 116 K and the zero resistivity critical temperature {T_c (R=0)} around 96, 86, 87, 78, and 77 K, for x=0, 0.015, 0.025, 0.05, and 0.075, respectively. The residual resistivity and normal state resistivity are increased from 0.397 Ω cm to 1.001 Ω cm and 0.17 Ω cm to 0.78 Ω cm for x=0 to 0.075. As the Y-content increases, much broader superconducting transitions, higher room temperature resistivity values and lower zero resistivity critical temperature values are observed. The suppression of superconductivity after Y-doping in $Cu_{0.5}Tl_{0.5}Ba_2(Ca_{2-x}Y_x)Cu_3O_{10-\delta}$ samples proposed that Y^{3+} creates correlated domains in between the CuO_2 planes and localizes the carriers. The mobility of the carriers along the c-axis is reduced due to localization of carriers across Y^{3+} in the material. The variation of superconductivity parameters depends upon the carriers concentration, their mobility, their homogeneity and separation between the conducting CuO_2 planes [15–17]. The suppression of superconductivity in $Cu_{0.5}Tl_{0.5}Ba_2(Ca_{2-x}Y_x)Cu_3O_{10-\delta}$ samples after Y-doping can also be elucidated from the reduction of carriers concentration and their mobility due to increase of anisotropy and decrease of inter-planes Josephson coupling with increasing Y-content in the material.

In order to investigate the effect of Y substitution on superconducting properties of $Cu_{0.5}Tl_{0.5}Ba_2(Ca_{2-x}Y_x)Cu_3O_{10-\delta}$ samples, we performed ac-susceptibility (χ) measurements. The real ($\chi^{/}$) and imaginary ($\chi^{//}$) components of ac-susceptibility of $Cu_{0.5}Tl_{0.5}Ba_2(Ca_{2-x}Y_x)Cu_3O_{10-\delta}$ samples are displayed in Fig. 5. The onset temperatures of diamagnetism in the above mentioned samples are observed around 99, 90, 96, and 88 K for x=0, 0.015, 0.025, and 0.05, respectively. The value of diamagnetism decreases with the increase of Y content in $Cu_{0.5}Tl_{0.5}Ba_2(Ca_{2-x}Y_x)Cu_3O_{10-\delta}$ samples. It shows that the transition temperature, defined as the temperature at which the Meissner signal begins to appear, decreases progressively with increasing Y content in the samples. The maximum peak of $\chi^{//}$ appears at a temperature (T_p), where the inter-granular field just penetrates the center of sample [18]. Two loss peaks can usually be seen in the imaginary part ($\chi^{//}$) of ac-susceptibility data: a broad peak at low temperature (coupling losses) and a narrower peak (intrinsic losses) near T_c^{onset} (K) but we did not see any intrinsic loss peak in our $Cu_{0.5}Tl_{0.5}Ba_2(Ca_{2-x}Y_x)Cu_3O_{10-\delta}$ samples. This may be due to small grains size and no considerable flux penetration can take place into the grains [19]. The overall ac-susceptibility curves are shifted to lower temperature values with increasing the Y content in the samples. The amplitude of $\chi^{//}$ is decreased with increasing Y content. The broadening of the peaks with increasing Y substitution can be due to gradual penetration of flux into the center of the inter-granular regions. The real and imaginary parts are zero ($\chi^{/}=\chi^{//}=0$), when the sample is in normal state (full penetration). The amplitude of $\chi^{//}$ falls down due to decreasing amount of flux penetration below T_p. When the temperature reaches to a certain lower value the whole body is shield. This indicated the destructive effect in the superconducting properties brought about by Y–Ca replacement in $Cu_{0.5}Tl_{0.5}Ba_2(Ca_{2-x}Y_x)Cu_3O_{10-\delta}$

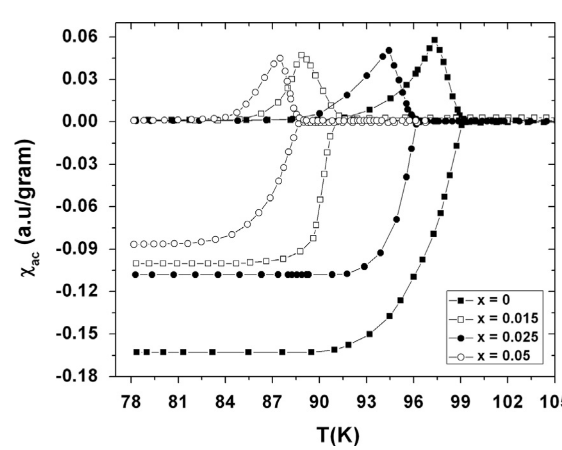

Fig. 5. The ac-susceptibility versus temperature measurement of $Cu_{0.5}Tl_{0.5}Ba_2(Ca_{2-x}Y_x)Cu_3O_{10-\delta}$ (x=0, 0.015, 0.025, and 0.05) superconductor samples.

samples [20–22]. If we look into the suppression of critical temperature and diamagnetism in the light of enhanced volume of the unit cell observed in the XRD measurements, it seems as if the density of mobile charge carriers has been suppressed with the incorporation of Y in the unit cell of $Cu_{0.5}Tl_{0.5}Ba_2(Ca_{2-x}Y_x)Cu_3O_{10-\delta}$ samples. It is most likely that the mobility of the carriers in the conducting CuO_2 planes is suppressed by doping of Y^{+3} at Ca^{+2} sites. The Y substitution at Ca sites is supposed to create coulomb-interactions induced distortions in the CuO_2 planes, creating correlated domains that would, at high Y substitution, end up in a static antiferromagnetic ordering. So the decrease of mobile carriers density in the conducting CuO_2 planes and their mobility result in the suppression of superconductivity in Y-doped $Cu_{0.5}Tl_{0.5}Ba_2(Ca_{2-x}Y_x)Cu_3O_{10-\delta}$ samples.

4. Conclusions

We have synthesized Y-doped $Cu_{0.5}Tl_{0.5}Ba_2(Ca_{2-x}Y_x)Cu_3O_{10-\delta}$ superconductor samples and studied their superconducting properties. The main objective of these experiments was to study the role of carriers and the influence of Y-doping on the mobility of the carriers in parallel and perpendicular to the conducting CuO_2 planes of $Cu_{0.5}Tl_{0.5}Ba_2(Ca_{2-x}Y_x)Cu_3O_{10-\delta}$ superconductor samples. The room temperature and residual resistivities are increased with the increase of Y content in $Cu_{0.5}Tl_{0.5}Ba_2(Ca_{2-x}Y_x)Cu_3O_{10-\delta}$ samples. The *c*-axis length and unit cell volume are increased by Y-doping. Hardening of apical and the softening of planar oxygen modes are the manifestation of Y^{3+} incorporation at Ca^{2+} sites in between the CuO_2 planes. The substitution of Y at Ca sites is supposed to create coulomb-interactions induced distortions in CuO_2 planes, creating correlated domains that would generate a static antiferromagnetic ordering. The substitution of Y might have weakened the inter-CuO_2-planes as well as inter-grain coupling leading to the deterioration of the microstructures and superconducting properties of $Cu_{0.5}Tl_{0.5}Ba_2(Ca_{2-x}Y_x)Cu_3O_{10-\delta}$ samples. Also, the Y substitution has deleterious effects on the mobility of the carriers that promote impeded motion of the carriers, which suppresses the superconducting properties of the material. It is most likely that Y^{+3} substituted at Ca^{+2} sites may reduce the Fermi vector, the Fermi velocity of the carriers and hence the superconducting properties of the material.

References

[1] Nawazish A. Khan, A.A. Khurrum, Enhanced superconducting properties of $Cu_{1-x}Tl_xBa_2Ca_{2-y}Mg_yCu_3O_{10-\delta}$ $y=0$, 0.5, 1.0, and 1.5, Applied Physics Letters 86 (2005) 152502.

[2] Nawazish A. Khan, G. Husnain, Superconductivity in Be substituted by Ca in $Cu_{0.5}Tl_{0.5}Ba_2Ca_{n-1-y}Be_yCu_nO_{2n+4-\delta}$ ($n=3$, 4 and $y=0.7$, 1.5, 1.7, 2.0), Physica C 436 (2006) 51.

[3] M. Mumtaz, Nawazish A. Khan, Improved interplane and intergranular coupling by Mg doping at Ca site in $Cu_{0.5}Tl_{0.5}Ba_2Ca_2(Cu_{0.5}Zn_{2.5})O_{10-\delta}$ superconductor, Journal of Applied Physics 103 (2008) 083913.

[4] Nawazish A. Khan, M. Zubair, M. Mumtaz, A.A. Khurram, Atmospheric pressure synthesis of Be- and Mg-doped $TlBa_2Ca_2Cu_3O_{10-\delta}$ superconductor, Ceramics International 39 (2013) 1901.

[5] C.S. Gopinath, S. Subramanian, P. Sumana Prabhu, M.S. Ramachandra Rao, G.V. Subba Rao, Structure, superconductivity and XPS studies of the $Bi_{2.1}Sr_{1.93}Ca_{0.97-x}Y_xCu_2O_{8+y}$ system, Physica C 218 (1993) 117.

[6] L. Manifacier, G. Collin, N. Blanchard, Correlations between crystallographic and physical properties in $(Bi, Pb)_2Sr_2(Ca, Y)Cu_2O_{8+\Delta}$ superconductors, Physica B 259–261 (1999) 562.

[7] K. Yamanaka, A. Suzuki, M. Suzuki, X.G. Zheng, Tunneling studies of pseudo and superconducting gaps in $Bi_2Sr_2Ca_{1-x}Y_xCu_2O_{8-y}$, Physica C 357–360 (2001) 237.

[8] S.M. Khalil, Effect of Y^{3+} substitution for Ca on the transport and mechanical properties of $Bi_2Sr_2Ca_{1-x}Y_xCu_2O_{8+\delta}$ system, Journal of Physics and Chemistry of Solids 64 (2003) 855.

[9] Y. Kunii, T. Suzuki, T. Gotoa, S. Nakajima, Anomalous longitudinal nuclear spin relaxation in $TlBa_2(Ca,Y)Cu_2O_7$ at the non-superconducting phase boundary, Journal of Magnetism and Magnetic Materials 272–276 (2004) e1521.

[10] E. Kandyel, Sol–gel synthesis, structural and superconducting properties of $(Hg_{1-y}Se_y)Sr_2(Y_{1-x}Ca_x)Cu_2O_{6+\delta}$, Journal of Solid State Chemistry 181 (2008) 3137.

[11] H. Sasakura, Y. Akagi, S. Tsukui, M. Adachi, New superconducting Pb-based 1212 cuprates containing boron, $(Pb_{0.5}B_{0.5})(Sr_{2-x}Ba_x)(Y_{1-y}Ca_y)Cu_2O_z$, Physica C 468 (2008) 925.

[12] Jeffrey C. De Vero, Glaiza Rose S. Blanca, Jaziel R. Vitug, Wilson O. Garcia, Roland V. Sarmago, Stoichiometric transfer of material in the infrared pulsed laser deposition of yttrium doped Bi-2212 films, Physica C 471 (2011) 378.

[13] Najamul Hassan, Nawazish A. Khan, Enhancement of superconducting properties in $Cu_{0.5}Tl_{0.5}Ba_2Ca_{0.5}M_{1.5}Cu_{1.5}Ni_{1.5}O_{10-\delta}$ (M=Mg, Be) superconductors, Materials Chemistry and Physics 112 (2008) 412.

[14] V. Mihalache, I.G. Deac, A.V. Pop, L. Miu, The pinning force density in polycrystalline $Bi_{1.8}Pb_{0.4}Sr_2Ca_{2-x}Y_xCu_3O_y$ multiphase systems, Current Applied Physics 11 (2011) 1010.

[15] A. Maeda, M. Hase, I. Tsukada, K. Noda, S. Takebayashi, K. Uchinokura, Physical properties of $Bi_2Sr_2Ca_{n-1}Cu_nO_y$ ($n=1$, 2, 3), Physical Review B 41 (1990) 6418.

[16] A.K. Santra, D.D. Sarma, C.N. Rao, Relation between the electronic structure and the superconductivity of cuprates as revealed by Cu 2p photoemission and theoretical investigations, Physical Review B 43 (1991) 5612.

[17] M. Mumtaz, Nawazish A. Khan, Anayat Ullah, Superconductivity in Co and Li substituted $Cu_{0.5}Tl_{0.5}Ba_2Ca_2Cu_{3-x}Co_xO_{10-\delta}$, Journal of Low Temperature Physics 163 (2011) 203.

[18] K.H. Muller, M. Nikolo, N. Savvides, R. Driver, Advances in Superconductivity, in: K. Kajimura, H. Hayakawa (Eds.), Springer, Tokyo, 1991, p. 119.

[19] K.H. Müller, S.J. Collocott, R. Driver, N. Savvides, AC susceptibility of granular superconductors, Superconductor Science and Technology 4 (1991) S325.

[20] A. Coskun, A. Ekicibil, B. Ozcelik, K. Kiymac, Field dependence of magnetization and dM/dH for Sm- and Gd-doped $Bi_{1.7}Pb_{0.3}Sr_2Ca_{2-x}RE_xCu_3O_{10+y}$ compounds, Chinese Physics Letters 21 (2004) 2041.

[21] S.K. Agarwal, B.V. Kumaraswamy, Low field AC susceptibility study of intergranular critical current density in Mg-substituted $CuBa_2Ca_3Cu_4O_{12-y}$ high temperature superconductors, Journal of Physics and Chemistry of Solids 66 (2005) 729.

[22] C. Terzioglu, D. Yegen, M. Yilmazlar, O. Gorur, M. Akdogan, A. Varilci, Investigation of Sm→Ca substitution in Bi(Pb)SrCaCuO high temperature superconductor by low field AC magnetic susceptibility, Journal of Materials Science 42 (2007) 4636.